Supporting Information

Energetic Stability and Its Role in the Mechanism of Ionic Transport in NASICON-type Solid State Electrolyte $Li_{1+x}Al_xTi_{2-x}(PO_4)_3$

Mykola Abramchuk[1], Albert A. Voskanyan[1], Yulia Arinicheva[2], Kristina Lilova[1], Tamilarasan Subramani[1], Qianli Ma[2], Enkhtsetseg Dashjav[2], Martin Finsterbusch[2] and Alexandra Navrotsky*[,1]

1) School of Molecular Sciences and Center for Materials of the Universe, Arizona State University, Tempe, AZ 85281, United States

2) Forschungszentrum Jülich GmbH, Institute for Energy and Climate Research, Materials Synthesis and Processing (IEK-1), 52425 Jülich, Germany

E-mail: Alexandra.Navrotsky@asu.edu

Materials and Methods

Synthesis

$Li_{1+x}Al_xTi_{2-x}(PO_4)_3$ powders (LATP, $0.1 \leq x \leq 0.5$) were prepared by an aqueous solution-based sol-gel method [1,2]. For the synthesis titanium (IV) isopropoxide ($Ti[OCH(CH_3)_2]_4$, 97%, Aldrich) was added into deionized water while stirring. The precipitate of titanium hydroxide was filtered and washed, and deionized water and nitric acid (65%, Aldrich) were then added to it. When a clear TiO^{2+} nitrate solution was formed, citric acid (double molar excess) was added to stabilize the solution. Stoichiometric amounts of lithium nitrate ($LiNO_3$, 99 %, Alfa Aesar) and aluminum nitrate nonahydrate ($Al(NO_3)_3 \cdot 9H_2O$, 99 %, Alfa Aesar) were weighed and added into the TiO^{2+} nitrate solution while stirring. After dissolution of both salts, a corresponding amount of ammonium dihydrogen phosphate ($NH_4H_2PO_4$, 99 %, Merck) was added to the solution leading to a sol formation. After 1 h, a stiff gel was spontaneously formed. The gel was dried at 353 K for 24 h. The dried gel was then calcined at 873 K for 3 h. The calcined powder was milled in ethanol with zirconia balls on a milling bench for 48 h. After drying, the powder was placed into a cylindrical pressing mold with a diameter of 13 mm and pressed under uniaxial pressure of 100 MPa. The pressed pellets were sintered for 5 h at 1323, 1273, 1223, 1173, and 1148 K for x = 0.1, 0.2, 0.3, 0.4, and 0.5, respectively. Additionally, the limiting composition with x = 0 ($LiTi_2(PO_4)_3$) was synthesized using conventional solid state reaction. The stoichiometric amounts of Li_2CO_3 (VWR International, Belgium, 99 %), TiO_2

(VWR International, Belgium, 99 %) and $NH_4H_2PO_4$, plus an excess of 20 wt.% Li to compensate its volatility, were mixed and homogenized in an agate mortar. The TiO_2 was preliminary dried at 873 K for 6 h. Then, the reaction mixture was transferred into a Pt crucible and slowly heated up with heating rate 120 K/h to 1273 K and kept there for 6 h in air and cooled down to room temperature with 300 K/h. After this calcination step, the sample was crushed, homogenized in a mortar and pressed to a pellet. During a second heat treatment, the pellet was sintered at 1273 K for 720 h in a corundum crucible on a powder bed of LATP.

Powder X-ray Diffraction and Optical Emission Spectroscopy

The phase purity and crystal structure of the sintered LATP powders was characterized by powder X-ray diffraction (PXRD) using a Bruker D4 Endeavor diffractometer with Cu-$K\alpha$ radiation using a step size of 0.02 ° at room temperature. The Rietveld refinements were performed by WinCSD software package [3]. The visualization of the crystal structure was done by VESTA [4]. PXRD patterns of all samples from this study are presented in Fig. S1.

Inductively coupled plasma optical emission spectroscopy (ICP-OES) (Thermo Elemental, IRIS Intrepid) was used to determine the elemental composition of the sintered LATP samples. For each experiment 10-30 mg of the LATP powders were mixed with 0.25 g sodium tetraborate and thermally treated at 1273 K in the muffle furnace for 0.5 h. The melts were dissolved in 30 mL HCl (5%) with the addition of 5 mL H_2O_2. The obtained solution was diluted to 50 mL by using distilled water. The experimental error for the ICP-OES analysis is 3 % of the detected concentration.

High-Temperature Oxide Melt Solution Calorimetry

To perform high-temperature oxide melt solution calorimetry (HTOMSC) studies, each LATP sample was pressed into pellets (m = 4-5 mg, d = 2 mm). The pellets were dropped from room temperature (298 K) into 20 g of molten sodium molybdate solvent ($3Na_2O \cdot 4MoO_3$) equilibrated at 1073 K inside a Tian Calvet twin calorimeter (AlexSYS, Setaram Cailure, France). The oxygen gas was bubbled through the solvent at 5 mL/min and flushed over the solvent at 90 mL/min to ensure the thorough mixing and complete dissolution of each sample. The drop experiments were repeated until at least eight successful drops with two standards error less than 1% between the enthalpy of drop solution (ΔH_{ds}) values were achieved. Prior to the drop solution experiments, the calorimeter was calibrated against the heat content of 5 mg pellets of corundum (α-Al_2O_3). To make

$3Na_2O \cdot 4MoO_3$ a stoichiometric mixture of sodium molybdate dihydrate ($Na_2MoO_4 \cdot 2H_2O$, 99.5%, Spectrum) and molybdenum (VI) oxide (MoO_3, 99.5%, Fisher Chemical), the starting materials were thoroughly ground in air and placed into a quartz crucible. The crucible was heated to 1073 K, kept at that temperature for 0.5 h, and then quenched in air. The experimental setup, fundamental physicochemical principles and methodology of the HTOMSC studies are described in detail elsewhere [5-7].

Drop solution enthalpy of Li$_2$O in sodium molybdate at 1073 K

ΔH_{ds} (Li_2O) was calculated using the experimentally measured drop solution enthalpy (ΔH_{ds}) of Li_2CO_3 (183.99 ± 0.33(8) kJ/mol), heat content of CO_2 [8], and formation enthalpy of Li_2CO_3 [9]. The thermochemical cycle is shown in Table S4. Before the drop solution experiments, the Li_2CO_3 was dried at 393 K for 24 h in air to remove traces of the moisture.

Energetics of mixing

In the main text, we presented experimental values of drop solution enthalpies for $Li_{1+x}Al_xTi_{2-x}(PO_4)_3$ along with the quadratic fit. Herein, we present the enthalpy of mixing ΔH_{mix}, the mixing entropy term ($T\Delta S_{mix}$) and the free energy of mixing ΔG_{mix} at 1200 K (Fig. S2) calculated using Eq. 2-4 from the main text. The calculation reveals positive values of ΔG_{mix} implying substantial deviation from the regular solution formalism.
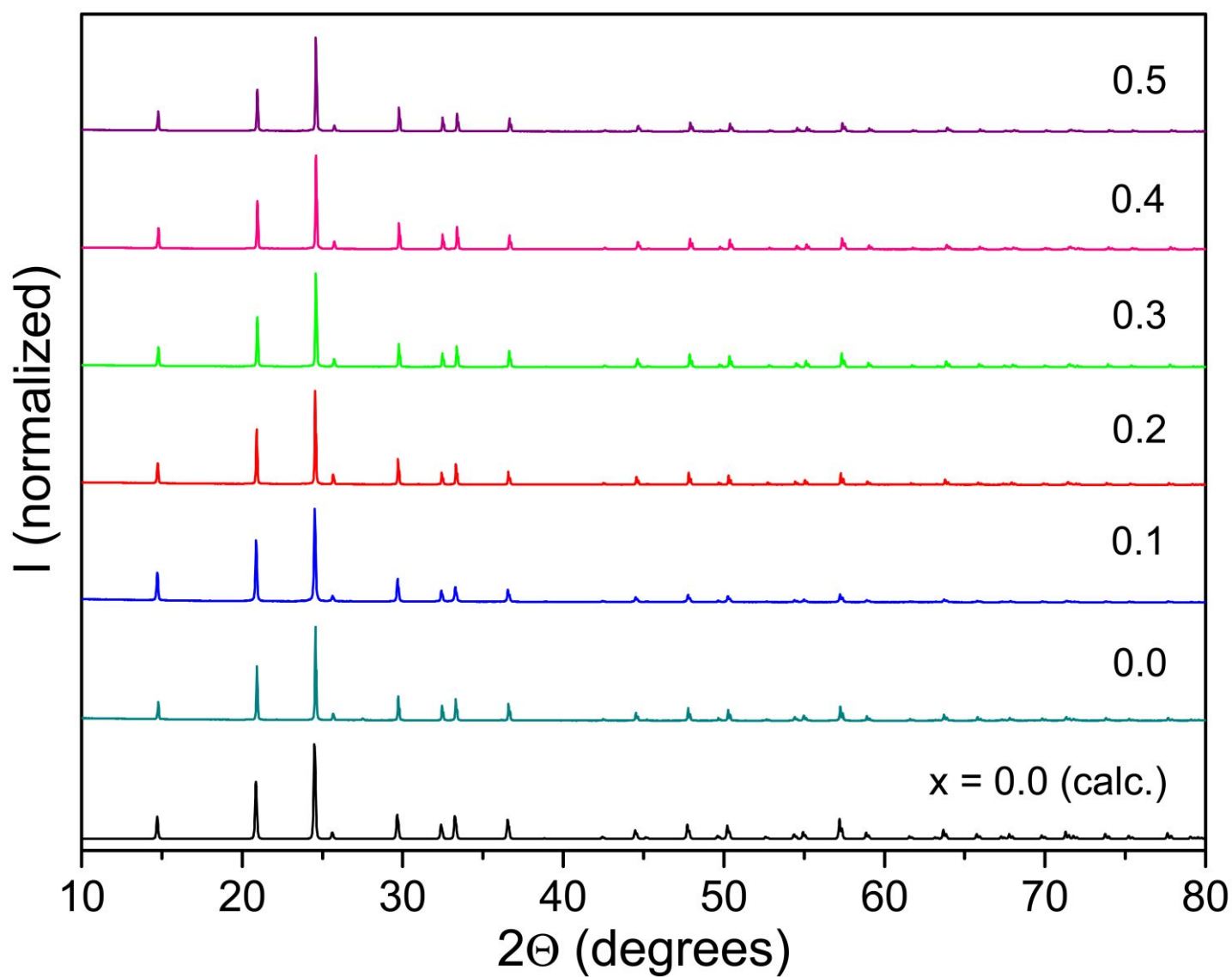
Figure S1. PXRD patterns of all LATP samples (0≤ x ≤ 0.5) used in the present study. A comparison with the calculated pattern for $LiTi_2(PO_4)_3$ (ICSD# 184088) highlights the absence of impurities.
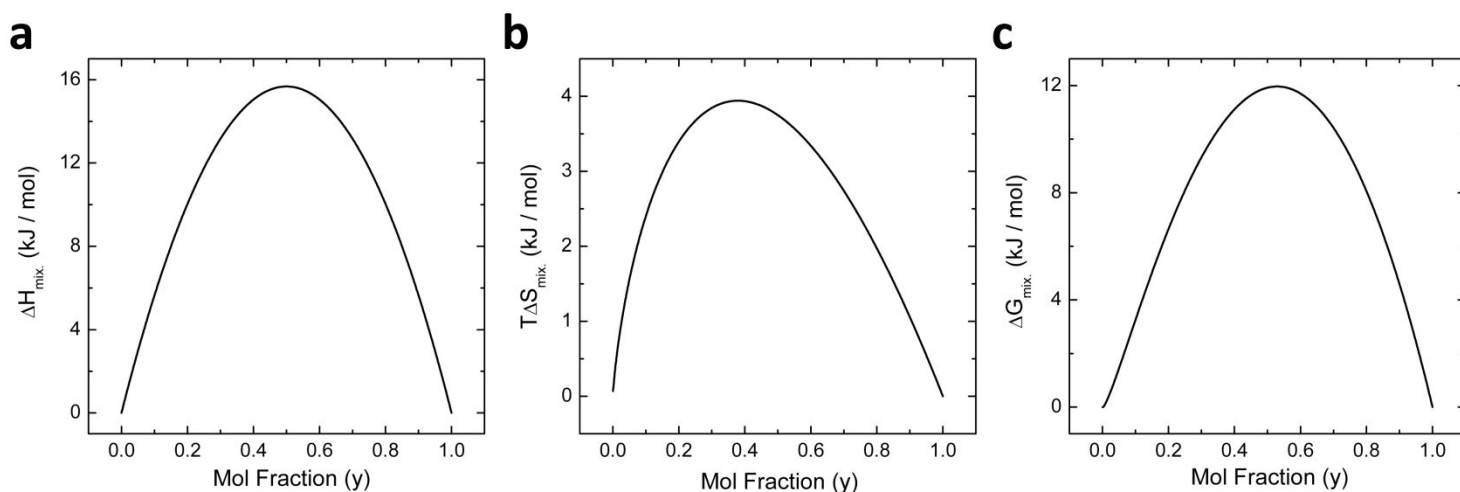
Figure S2. Enthalpy of mixing (a), the mixing entropy term (b) and the free energy of mixing for the solid solution $Li_{1+y/2}Al_{y/2}Ti_{2-y/2}(PO_4)_3$ (y = 2x).

Table S1. Chemical composition and crystallographic data for $Li_{1+x}Ti_{2-x}Al_x(PO_4)_3$.

Composition (x)	0.0	0.1	0.2	0.3	0.4	0.5
ICP OES (x)	-	0.10	0.18	0.29	0.37	0.47
Space group	$R\bar{3}c$	$R\bar{3}c$	$R\bar{3}c$	$R\bar{3}c$	$R\bar{3}c$	$R\bar{3}c$
a (Å)	8.51279(6)	8.50665(7)	8.50371(5)	8.49963(4)	8.49492(5)	8.48979(3)
c (Å)	20.8661(3)	20.8367(4)	20.8139(2)	20.7939(2)	20.7780(2)	20.7617(2)
V (Å³)	1309.53(4)	1305.80(5)	1303.47(3)	1300.97(2)	1298.54(2)	1295.95(2)
Z	6	6	6	6	6	6
$D_{calc.}$ (g/cm³)	2.9491(1)	2.9470(1)	2.9413(1)	2.9364(1)	2.9313(1)	2.9262(1)
T (K)	295	295	295	295	295	295
R_I	0.0282	0.0422	0.0499	0.0325	0.0321	0.0373
R_p	0.0466	0.0356	0.0382	0.0400	0.0420	0.0431
R_{wp}	0.0729	0.0479	0.0523	0.0548	0.0571	0.0591

Table S2. Experimental drop solution enthalpies, and enthalpies of formation of the $Li_{1+x}Ti_{2-x}Al_x(PO_4)_3$ at 298 K.

Nominal (x)	ΔH_{ds} (kJ/mol)	$\Delta H^o_{f,ox}$ (kJ/mol)	$\Delta H^o_{f,el}$ (kJ/mol)
0.00	391.88±3.65(9)	-507.54±6.86	-4951.68±9.35
0.10	384.81±3.39(9)	-506.16±6.74	-4969.58±9.23
0.20	384.55±3.47(10)	-511.60±6.97	-4994.32±9.46
0.30	378.73±2.51(12)	-511.47±6.15	-5013.47±8.64
0.40	393.78±5.21(13)	-532.21±9.00	-5053.50±11.49
0.50	399.52±3.81(8)	-543.65±7.74	-5084.23±10.23

Error represents two standard deviations of the mean, and value in () is the number of drop experiments performed.

Table S3. Thermodynamic cycle used to calculate the enthalpies of formation of $Li_{1+x}Ti_{2-x}Al_x(PO_4)_3$ from elements.

Eq.	Reaction	Heat effect
I	2Li (s, 298 K) + 1/2O$_2$(g, 298 K) → Li$_2$O (s, 298 K)	$\Delta H^o_{f,el}$ (Li$_2$O) [10]
II	Ti (s, 298 K) + O$_2$ (g, 298 K) → TiO$_2$ (s, 298 K)	$\Delta H^o_{f,el}$ (TiO$_2$) [11]
III	2Al (s, 298 K) + 3/2 O$_2$ (g, 298 K) → Al$_2$O$_3$ (s, 298 K)	$\Delta H^o_{f,el}$ (Al$_2$O$_3$) [11]
IV	2P (s, 298 K) + 5/2 O$_2$ (g, 298 K) → P$_2$O$_5$ (s, 298 K)	$\Delta H^o_{f,el}$ (P$_2$O$_5$) [8]
V	(1+x)/2 Li$_2$O (s, 298 K) + (2-x) TiO$_2$ (s, 298 K) + x/2 Al$_2$O$_3$ (s, 298 K) + 3/2 P$_2$O$_5$ (s, 298 K) → Li$_{1+x}$Ti$_{2-x}$Al$_x$P$_3$O$_{12}$ (s, 298 K)	$\Delta H_{f,ox}$ (LATP)
VI	(1+x) Li (s, 298 K) + (2-x) Ti (s, 298 K) + x Al (s, 298 K) + 3 P (s, 298 K) + 6O$_2$ (g, 298 K) → Li$_{1+x}$Ti$_{2-x}$Al$_x$P$_3$O$_{12}$ (s, 298 K)	$\Delta H_{f,el}$ (LATP)
VII	$\Delta H_{f,el}$ = (1+x)/2ΔH^o_f (Li$_2$O) + (2-x) ΔH^o_f (TiO$_2$) + x/2 ΔH^o_f (Al$_2$O$_3$) + 3/2 ΔH^o_f (P$_2$O$_5$) + $\Delta H_{f,ox}$	

Table S4. Thermodynamic cycle used to calculate the drop solution enthalpy of Li_2O in sodium molybdate ($3Na_2O \cdot 4MoO_3$) at 1073 K.

Eq.	Reaction	Heat effect
I	Li_2CO_3 (s, 298 K) → Li_2O (soln, 1073 K) + CO_2 (g, 1073 K)	$\Delta H_{ds,1}$ = 183.99 ± 0.33(8) kJ/mol
II	Li_2O (s, 298 K) → Li_2O (soln, 1073 K)	$\Delta H_{ds,2}$ = -77.21 ± 2.44 kJ/mol
III	CO_2 (s, 298 K) → CO_2 (g, 1073 K)	$\Delta H_{CO2} = \int_{298}^{1073} C_p dT$
IV	Li_2O (s, 298 K) + CO_2 (g, 298 K) → Li_2CO_3 (s, 298 K)	ΔH^o_f (Li_2CO_3) = - 223.79 ± 2.11 kJ/mol
V	$\Delta H_{ds,2} = \Delta H^o_f (Li_2CO_3) + \Delta H_{ds,1} - \Delta H_{CO2}$	

References

[1] E. Dashjav, Q. Ma, Q. Xu, C.-L. Tsai, M. Giarola, G. Mariotto and F. Tietz, "The influence of water on the electrical conductivity of aluminum-substituted lithium titanium phosphates," *Solid State Ion.* **2018**, *321*, 83-90.

[2] Q. Ma, Q. Xu, C. Tsai, F. Tietz and O. Guillon, "A Novel Sol–Gel Method for Large-Scale Production of Nanopowders: Preparation of $Li_{1.5}Al_{0.5}Ti_{1.5}(PO_4)_3$ as an Example," *J. Am. Ceram. Soc* **2016**, *99*, 410-414.

[3] L. Akselrud and Y. Grin, "WinCSD: software package for crystallographic calculations (Version 4)," *J. Appl. Crystallogr.* **2014**, *47*, 803-805.

[4] K. Momma and F. Izumi, "VESTA 3 for three-dimensional visualization of crystal, volumetric and morphology data," *J. Appl. Crystallogr.* **2011**, *44*, 1272–1276.

[5] A. Navrotsky, "Progress and new directions in high temperature calorimetry," *Phys. Chem. Miner.* **1977**, *2*, 89–104.

[6] A. Navrotsky, "Progress and new directions in high temperature calorimetry revisited," *Phys. Chem. Miner.* **1997**, *24*, 222-241.

[7] A. Navrotsky, "Progress and New Directions in Calorimetry: A 2014 Perspective," *J. Am. Ceram. Soc.* **2014**, *97*, 3349–3359.

[8] R. A. Robie and B. S. Hemingway, Thermodynamic properties of minerals and related substances at 298.15 K and 1 bar (10^5 pascals) pressure and at higher temperatures, Washington, DC: United States Government Printing Office, **1995**.

[9] M. W. Chase, Jr., C. A. Davies, J. R. Downey, Jr., D. J. Frurip, R. A. McDonald, A. N. Syverud, "JANAF Thermochemical Tables, Vol. 14, 3rd ed.," American Chemical Society and American Institute of Physics, **1985**.

[10] G. K. Johnson, R. T. Grow and W. N. Hubbard, "The enthalpy of formation of lithium oxide (Li_2O)," *J. Chem. Thermodyn.* **1975**, *7*, 781-786,.

[11] S. Hayun, S. Salhov, K. Lilova and A. Navrotsky, "Enthalpies of Formation of High Entropy and Multicomponent Alloys using Oxide Melt Solution Calorimetry," *Intermetallics* **2020**, *125*, 106897.